Bimetallic Molecular Catalyst Design for Carbon Dioxide Reduction

Philipp Gotico, Zakaria Halime, Winfried Leibl, Ally Aukauloo

REVIEW

Bimetallic Molecular Catalyst Design for Carbon Dioxide Reduction

Philipp Gotico,*[a] Zakaria Halime,[b] Winfried Leibl,[a] Ally Aukauloo*[a],[b]

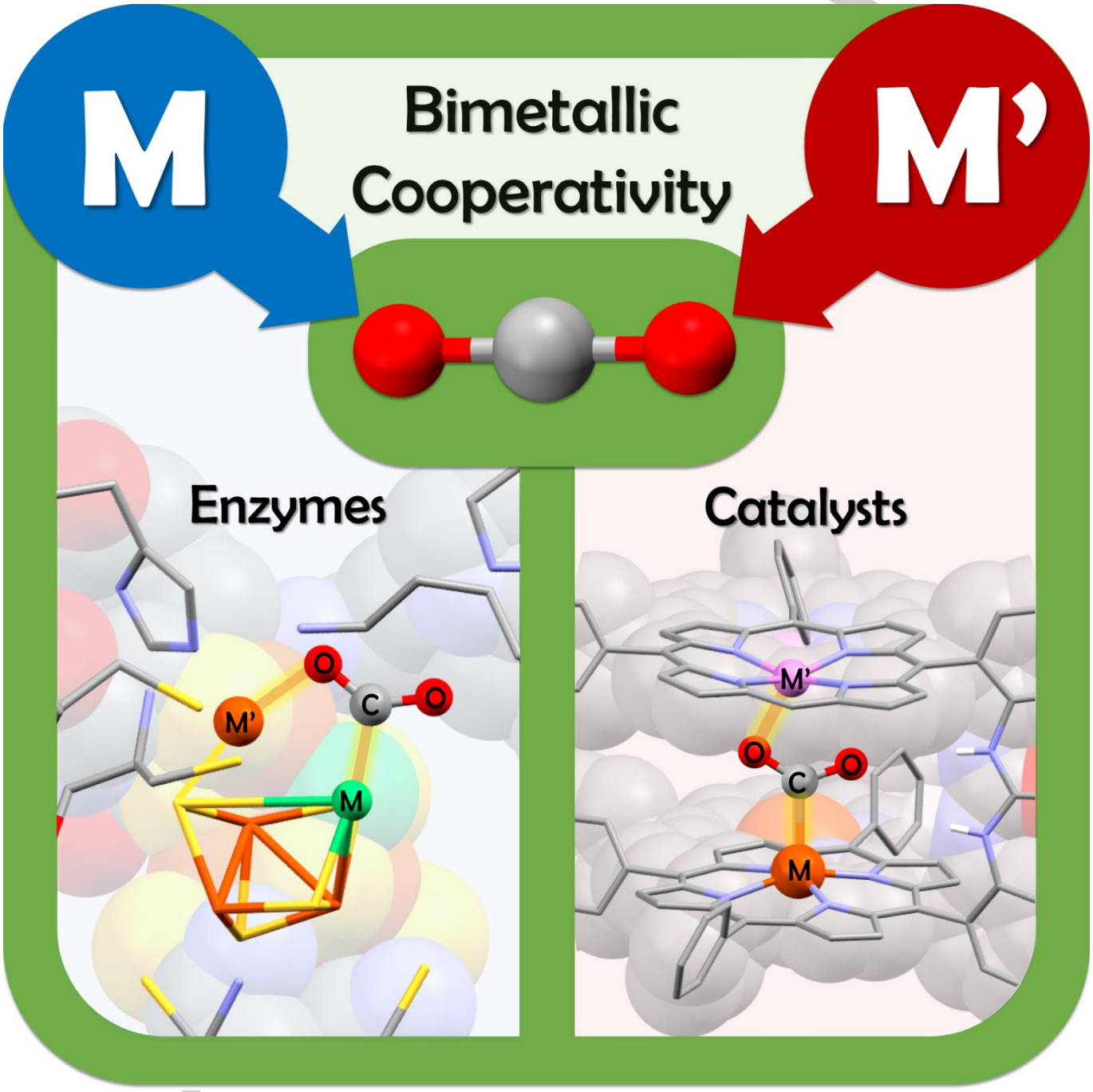

[a] Dr. P. Gotico, Dr. W. Leibl, Prof. A. Aukauloo
Université Paris Saclay
CEA, CNRS, Institute for Integrative Biology of the Cell
91198 Gif Sur Yvette, France
E-mail: philipp.gotico@cea.fr, ally.aukauloo@universite-paris-saclay.fr
[b] Dr. Z. Halime, Prof. A. Aukauloo
Université Paris Saclay
CNRS, Institut de Chimie Moléculaire et des Matériaux d'Orsay
91405 Orsay, France

Abstract: The core challenge in developing cost-efficient catalysts for carbon dioxide (CO_2) conversion mainly lies in controlling its complex reaction pathways. One such strategy exploits bimetallic cooperativity, which relies on the synergistic interaction between two metal centers to activate and convert the CO_2 substrate. While this approach has seen an important trend in heterogeneous catalysis as a handle to control stabilities of surface intermediates, it has not often been utilized in molecular and heterogenized molecular catalytic systems. In this review, we gather general principles on how natural CO_2 activating enzymes take advantage of bimetallic strategy and how phosphines, cyclams, polypyridyls, porphyrins, and cryptates-based homo- and hetero-bimetallic molecular catalysts can help understand the synergistic effect of two metal centers.

1. Introduction and Scope

The development of cost-efficient catalysts for the selective carbon dioxide (CO_2) reduction using renewable energy sources is an urgent requirement to address the colossal task of returning CO_2 to energy-rich molecules. It can easily be comprehended that to achieve such a conversion on a massive scale, heterogeneous catalysis for CO_2 reduction will undoubtedly be at work. This research field has shown encouraging perspectives in the fabrication of novel solid state catalysts and in the control of important adsorbates to tune CO_2 reduction product selectivity.[1,2] One of the few strategies to realize this makes use of two-metal cooperativity which has been recently shown useful not just in controlling CO_2 reduction selectivity[3,4] but also for nitrite reduction,[5] proton reduction,[6,7] oxidation reactions,[8,9] CO_2 fixation reactions,[14,15] sensing,[16,17] purification,[18] other catalytic reactions,[10–13] and environmental applications.[19,20] In order to attain such catalytic materials, not only complex synthetic tactics are needed but in addition, these reactive surfaces might be chemically altered during the catalytic cycle. An elegant way to counter such modifications resides in the design of molecular catalysts that provide several synthetic handles for the structural and topological control of two metal centers through ligand design. A fundamental asset of molecular catalysts is the access they provide to the understanding of the catalytic mechanisms using a large set of spectroscopic methods to probe the multi electron and proton processes.

The bimetallic systems work cooperatively to store charges and to activate the CO_2 substrate. In a classical push-pull donor-acceptor scenario, one metal center acts as a Lewis base to transfer an electron pair to the coordinated CO_2 molecule while the second metal center acts as a Lewis acid to promote C–O bond cleavage and the formation of CO (Scheme 1). Similar scenarios can promote the production of formates and oxalates depending on how the CO_2 substrate is activated by the metal ions. Furthermore, the premise of a tandem reaction can be realized with bimetallic strategy where one of the metal ions is envisioned to transfer critical intermediates to the other to form further reduced C_1 and C_2 products.[21–23]

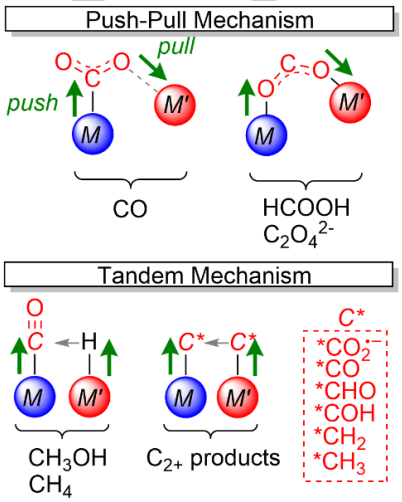

Scheme 1. The potential of bimetallic strategy in activating and converting CO_2.

To date, the rare publications on bimetallic activation in molecular and heterogenized molecular catalytic systems were focused mainly on the electroreduction of CO_2 to CO. However, examples of C-C bond formation leading to oxalate and further reduced products such as methane have been discovered. Henceforth, it is timely to gather the general principles of the functioning of natural bimetallic enzymes and implement them in synthetic systems to provide key understandings in the general field of catalysis.

We refer the reader to recent reviews on a related theme where chemists are manipulating the second coordination sphere effects such as local proton sources, hydrogen bond donors, and electrostatic activators to enhance the catalytic activity of molecular complexes.[24–27] A recent review from the group of Zhong and Lu presented the use of bimetallic molecular catalysts in artificial photosynthesis, where most efforts are designed for water and oxygen activating catalysts based on inspirations from the multi-metallic Mn_4Ca cluster of the oxygen evolving complex and from cytochrome *c* oxidase complexes.[28] Herein, we extend and update the understanding in the activation and conversion of carbon dioxide, looking initially at how natural CO_2 activating enzymes take advantage of bimetallic strategy and then going to artificial catalysts that make use of the lessons and understanding of the active sites in natural systems.

2. Bimetallic CO_2 activation in nature

In nature, there are six pathways known to fix carbon dioxide as organic material for biomass. They involve enzymes performing carboxylation of various sugars, synthesis of acetyl coenzyme-A, and reduction of CO_2 (to CO or formate).[29] Among these, bimetallic CO_2 activation was only observed in CO dehydrogenase (CODH) that catalyzes the two-electron, two-proton interconversion between CO_2 and CO. Two types of CODH exist: one from anaerobic microorganisms such as *Moorella thermoacetica*, *Carboxydothermus hydrogenoformans*, and *Methanosarcina barkerii* with a [NiFe] active site, and another from aerobic organisms such as *Oligotropha carboxidovorans* with a [MoCu] active site.[29]

The [NiFe] CODH (Scheme 2) catalyzes the reversible reduction of CO_2 to CO with turnover frequency (TOF) of 45 s^{-1} for CO_2 reduction and TOF of 40,000 s^{-1} for CO oxidation.[30] Crystallographic studies of the oxidized form of this [NiFe] C cluster site show a Ni center taking the place of one Fe atom of an Fe_4S_4 cluster and positioned in close proximity to the displaced forth Fe (Scheme 2, structure **1**). Whether this modified configuration plays similar roles as that of iron-sulfur clusters in other natural systems,[31,32] or has a specific function in CODH is yet to be fully confirmed. The Ni species is coordinatively unsaturated binding three sulfur ligands in a distorted T-shaped configuration. In its reduced form (reaction with Ti^{III} citrate) and in the presence of CO_2 substrate (through bicarbonate ion source), CO_2 is observed to bridge the Ni and Fe metals, as shown in structure **3**. CO_2 is bound to a reduced formal $Ni^{"0"}$ metal center (presumed oxidation state change after two-electron reduction at –600 mV) through the C atom completing the square planar coordination of the Ni while one of carboxylate's oxygen atoms is bound to the pendent Fe atom.[33] The same oxygen atom forms a hydrogen bond with a lysine (Lys_{563}) residue.

This bimetallic activation, reminiscent of a frustrated Lewis base (Ni) – Lewis acid (Fe) pair, works in synergy with the second coordination sphere activation to cause only minor changes from the T-shaped coordination geometry to square planar.[33] This structure promotes the heterolytic cleavage of the C-O bond, resulting in a CO coordinated to the Ni metal and a hydroxide coordinated to the Fe metal. The CO is then released from this Ni center to form back the oxidized state, closing the proposed catalytic cycle.[29] The low reorganizational energy observed from these experimentally determined structures also participates to the high turnover rates of the enzyme at a potential near the thermodynamic value for CO_2 to CO reduction.[34] The stabilization of the reactive intermediates through multiple hydrogen bonding and electrostatic interactions also participates in the catalytic performance of the enzyme.

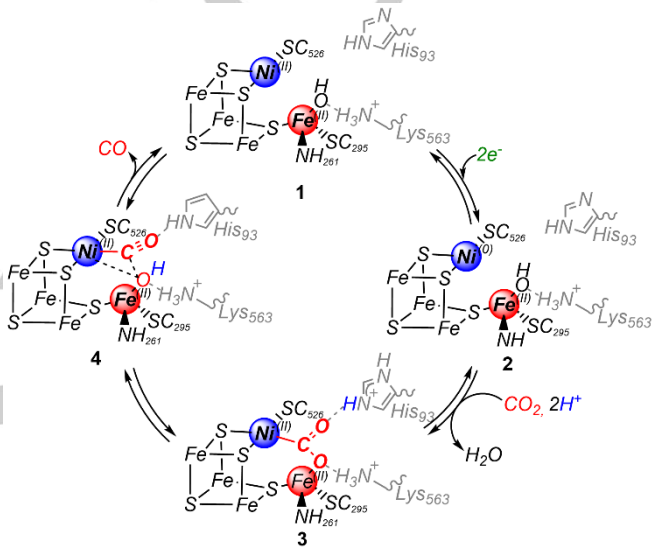

Scheme 2. Proposed structure-based mechanism for the catalytic cycle of [NiFe] CODH for the reversible reduction of CO_2 to CO. Adapted from Ref. 33, Copyright © 2007, The American Association for the Advancement of Science.

Philipp Gotico received his PhD in Chemistry at the French Alternative Energies and Atomic Energy Commission (CEA) focused on molecular catalyst design and characterization. After postdoctoral stints at the Institute of Molecular Sciences of Orsay (France) and Helmholtz Zentrum Berlin (Germany), he joined back his former lab in CEA as a Senior Researcher working on bio-inspired catalysis and hybrid interfaces.

Zakaria Halime received his PhD in Chemistry from the University of Rennes 1, France. After a postdoctoral experience in Karlin's group at Johns Hopkins University (USA), and Fukuzumi's group at Osaka University (Japan), he was appointed as a Senior Researcher at CNRS and University Paris Saclay where he is currently working on the catalytic transformation of small molecules into sustainable fuels.

Winfried Leibl obtained his PhD from the University of Osnabrück, Germany. He joined the biophysics group at CEA Saclay (France) with a postdoctoral fellowship to work on primary events in natural photosynthesis before being appointed a Senior Researcher position at the same Institute. He is currently heading a group focused on functional characterization of natural and artificial photocatalytic systems.

Ally Aukauloo obtained his PhD from Université de Bourgogne on porphyrin isomers. He started as an associate professor in the field of molecular magnetism and then shifted to bioinorganic chemistry focussing on Artificial Photosynthesis. He is currently full professor at University Paris Saclay, a research collaborator at the CEA Saclay, and a senior member of the Institut Universitaire de France.

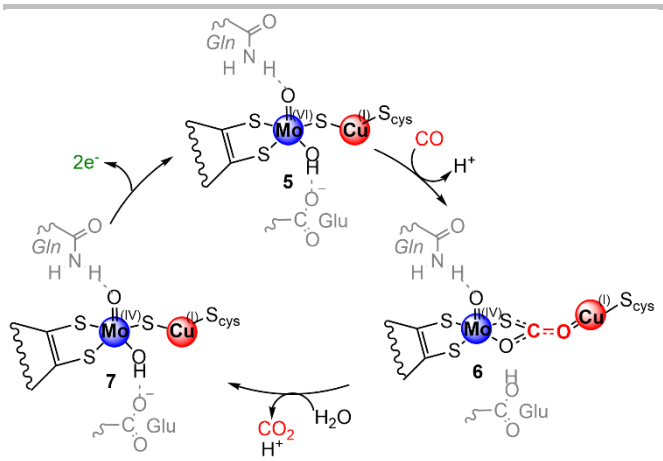

Scheme 3. Proposed structure-based mechanism for the catalytic cycle of [MoCu] CODH towards oxidation of CO to CO_2. Adapted from Ref. 35, Copyright © 2002, The National Academy of Sciences, U.S.A. PNAS is not responsible for the accuracy of this translation.

[MoCu] CODH (Scheme 3) has a similar structure as the [NiFe] CODH with the presence of a heterobimetallic metal center in the active site, though it was observed to only catalyze the oxidation of CO to CO_2 at a much lower TOF of 100 s^{-1}.[35,36] The oxidized form of the active site shows a Mo metal ion with an apical oxo group linked to two sulfur atoms of the molybdopterin cytosine dinucleotide cofactor, as shown in structure **5**. The second coordination sphere similarly contains amino acid residues such as glutamine and glutamate that are within hydrogen bonding distances from the oxo and hydroxyl ligands, respectively. Based on n-butylisonitrile-inhibited enzyme studies,[35] the reaction of a Mo^{VI} oxo/hydroxy species with CO leads to the formation of the reduced Mo^{IV} state with a thiocarbonate insertion product, structure **6**. This is a distinct difference with regard to the [NiFe] CODH as the carbon atom of the carboxylate-like intermediate is bound to the ligated sulfido group acting as the Lewis base, instead of the reduced Mo metal center.[29]

These enzymes involved in CO_2/CO interconversion seemingly contain similar features. First, they consist of sulfur-rich ligand structures that can store and supply electrons (Fe_3S_4 cluster, and pterin-like cofactors). Second, they employ a substrate-activating environment either by bimetallic Lewis acid-base pair or by second coordination sphere activation from nearby amino acid residues. Of note, in both cases, only one of the metal ions acts as a redox shuttle (Ni, Mo) while the other remains in its unchanged oxidation state (Fe, Cu). Third, they promote good CO_2 binding in meticulously pre-organized active sites with minimal changes in the geometry, resulting in low reorganizational energies. Lastly, they take advantage of the intrinsic water channels within the protein matrix to manage the proton convoy and promote proton-coupled electron transfer steps, significantly decreasing the thermodynamic requirement of the reactions. Interestingly, these discrete two-electron steps are also involved in the eight-electron reduction reactions observed for methanogenic archaea catalyzing reduction of CO_2 to methane and for acetogenic bacteria catalyzing reduction of CO_2 to acetic acid.[37] As such, fundamental lessons from the biological two-electron reduction in CODH would be particularly interesting in designing synthetic CO_2 reduction catalysts.

3. Molecular Bimetallic Catalysts

Early synthetic models of the CODH C-cluster have been extensively investigated by the group of Holm even before the advent of the protein X-ray structures. They successfully synthesized a series of [$NiFe_3S_4$] cubane models mimicking the active site of CODH[38,39] and bimetallic NiFe analogues complexes with the focus on the two metal ions that are intimately involved in the activation and catalytic bond breaking and making process.[40] However, there were no mentions of the catalytic activity of such bioinspired models. This is a common roadblock in the design of molecular catalysts where structural features do not necessarily match the catalytic activity. Another such example comes from structural mimics of the bimetallic active sites of hydrogenases to develop synthetic catalysts towards reversible reduction of protons to hydrogen.[41] It is noteworthy that such systems provide considerable insights in the electronic properties of the biomimetic models. As a matter of fact, to reach catalytic systems, chemists take profit of the orchestration of chemical functions in ligand design to shape the reactivity pattern of molecular complexes and to further improve the existing catalytic platforms: phosphines, cyclams and other aza-macrocyclic complexes, polypyridyl complexes (*e.g.*, bipyridines, phenanthrolines, terpyridines, quaterpyridines, etc.), and metallo-porphyrins, -phthalocyanines, and -corroles. The addition of chemical functionalities in the second coordination shell to establish local proton sources, hydrogen bond relays, and electrostatic activators in the vicinity of the active site has led to unprecedented enhancement in the catalytic properties.[24–27] Herein, we take a closer inspection to the rarely investigated bimetallic strategy (*homo- vs hetero*-bimetallic) in activating and reducing CO_2.

3.1. Homobimetallic Design

3.1.1. Phosphine based catalysts

The first reported bimetallic CO_2 reduction catalyst dated back to 1987 and the work of the group of Kubiak with a bimetallic 'cradle' nickel phosphine complex (catalyst **8a**, Figure 1).[42] The catalyst operates at a potential as low as −0.67 V *vs* NHE. When it reacts with CO_2 to produce structure **8b**, it shows no direct cooperativity of the two metals in activating the CO_2 substrate. Extended exposure to pressurized CO_2 shows complete carbonylation of the catalyst forming the CO cradle complex **8c**, where the carbonyl groups are now cooperatively stabilized by the Ni metals. This, however, leads to poisoning of the system and intriguingly, labelling studies suggested that these CO groups did not come from CO_2. Further modifications in catalyst **9** still suffers from similar poisoning by the reaction product (CO), only achieving an estimated turnover frequency (TOF) of 1.0 s^{-1}.[43]

Palladium phosphine complexes, pioneered by the group of DuBois in 1991, have been shown to be highly active catalysts for CO_2 reduction to CO at low overpotentials.[44] They suffer, however, from slow CO_2 binding, which was considered the rate-determining step in the catalytic cycle. A bimetallic Pd catalyst with methylene linker was synthesized (catalyst **10a**)[45] to increase the affinity for CO_2. It similarly mimics the activation in CODH with a seven membered CO_2 adduct structure **10b** (bold bonds). This results in a three orders of magnitude higher rate constant compared to the monometallic analogue. However, the

system displays a low turnover number (TON) of 8 during electrolysis at −0.67 V *vs* NHE in dimethylformamide (DMF) with 0.1 M HBF_4. This was explained by the formation of a Pd(I)-Pd(I) bond shown in structure **10c** which significantly reduces catalyst lifetime. A more rigid *meta*-phenyl linker in catalyst **11** was attempted to prevent the dimer formation but it resulted in a lack of cooperative effects as the catalytic rates were comparable to the monometallic analogue.[46]

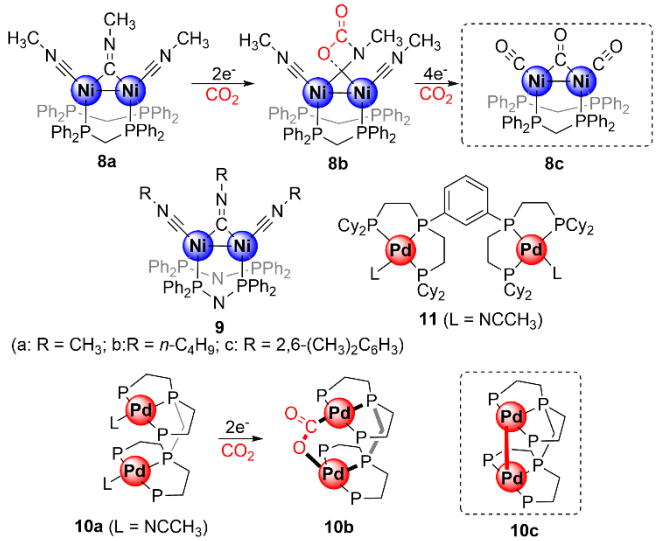

Figure 1. Phosphine ligand based homobimetallic catalysts.

3.1.2. Cyclam based catalysts

After discovering the selective CO_2 to CO electrocatalytic activity of Ni-cyclam in water (where cyclam denotes 1,4,8,11-tetraazacyclotetradecane),[47] the group of Collin and Sauvage reported in 1988 a bimetallic Ni_2(biscyclam)$^{4+}$ complex (catalyst **12**, Figure 2).[48] The catalyst was electrocatalytically active in reducing CO_2 to CO in water with a Faradaic efficiency (FE) of 93%. Interestingly, formate was produced in DMF with 0.1 M H_2O (68% FE at −1.16 V *vs* NHE). Unfortunately, the bimetallic catalyst shows much lower performance than its monometallic analogue in terms of both current density and selectivity. This was explained by the lower surface coverage of the adsorbed coplanar catalyst in which only one of the Ni sites is active.

A methylated analogue, catalyst **12b**, was consequently reported by the group of Mochizuki which showed an improved photocatalytic CO_2 reduction to CO compared to the monometallic analogue when coupled with a Ru photosensitizer (PS) and ascorbic acid as a sacrificial electron donor (SED).[49] Unfortunately, no electrochemical data was given to show distinct differences nor was any experimental evidence for cooperativity. This might stem from the long separation of 8.3 Å between the coplanar Ni cyclam sites based on the X-ray crystal structure. Indeed, a systematic study by the group of Crayston on the linker length of similar cofacial arranged Ni cyclams (catalyst **13** and **14**), showed poorer electrocatalytic performance of the bimetallic catalysts compared to their monometallic counterpart.[50]

To better control the distance between the two metals, in 2018, the group of Zhong and Lu synthesized catalyst **15a** where the Ni cyclam units are linked by a more rigid *ortho*-phenyl spacer, compelling a cofacial configuration.[51] This catalyst showed 95% FE (0.6 mA cm^{-2}) towards CO and a TOF of 190 s^{-1} at −1.16 V *vs* NHE in acetonitrile (CH_3CN) with 11 M H_2O. The cooperativity between the two metals was evidenced by the better performance of catalyst **15a** compared to the monometallic analogue (FE of 62%, 0.42 mA cm^{-2}) or the coplanar bimetallic analogue **16** connected through a *para*-phenyl spacer (FE of 25%, 0.4 mA cm^{-2}). Density Functional Theory (DFT) calculations show that the improvement is due to the through-space stabilization between the partial negative charge on the COO species bound to one Ni and the positive charge of the other Ni (structure **15b**). Interestingly, unlike in the CODH active site, the CO_2 adduct still maintains a linear structure, possibly pertaining to the lower extent of activation in these cofacial Ni cyclams.

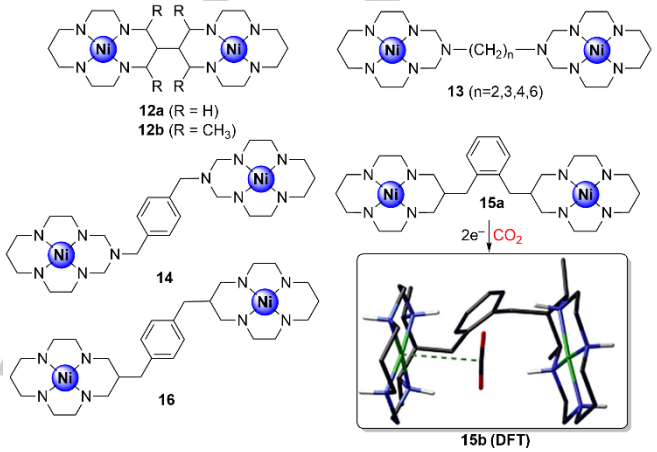

Figure 2. Cyclam ligand based homobimetallic catalysts. Structure 15b reproduced from Ref. 51 with permission from the Royal Society of Chemistry.

3.1.3. Polypyridyl based catalysts

Though copper has been heavily studied for heterogeneous catalysis for CO_2 reduction due to its inherent ability to go beyond the simple 2-electron reduction product,[52] it is rarely studied in a molecular bimetallic scheme. In 1994, the group of Haines and Kubiak first reported a bimetallic copper (II) complex with a PPh_2bpy ligand [6-(diphenylphosphino)-2,2'-bipyridyl)], catalyst **17** in Figure 3.[53] The catalyst reductively disproportionates two molecules of CO_2 to produce $CO_3^{2-}$and CO, with a TOF of only 2 h^{-1}. However, the mechanism is hypothesized to involve only one Cu metal to form a CO_2 adduct, without providing the intended cooperativity between the two metals. A much more successful feat was reported by the group of Bouwman with bimetallic copper (I) catalyst **18a** with N-(2-mercaptopropyl)-N,N-bis(2-pyridylmethyl)amine ligand.[54] The catalyst is immediately oxidized by CO_2 from air to form a tetranuclear copper (II) complex containing two bridging CO_2-derived oxalates (structure **18b**). The oxalate is quantitatively released upon reaction with a lithium salt and application of a potential of −0.03 V *vs* NHE regenerates the starting complex. A TON of six for a 7-hour catalysis has been demonstrated. Extra care must be given to confirm product origin because in another bimetallic Cu polypyridyl complex, oxalate was found to come from the oxidation of ascorbate, and not from the reduction of CO_2.[55] The rarity of reports on such dicopper molecular system brings opportunities for further studies, especially since it could shed light on the selectivity control of metallic copper surfaces.

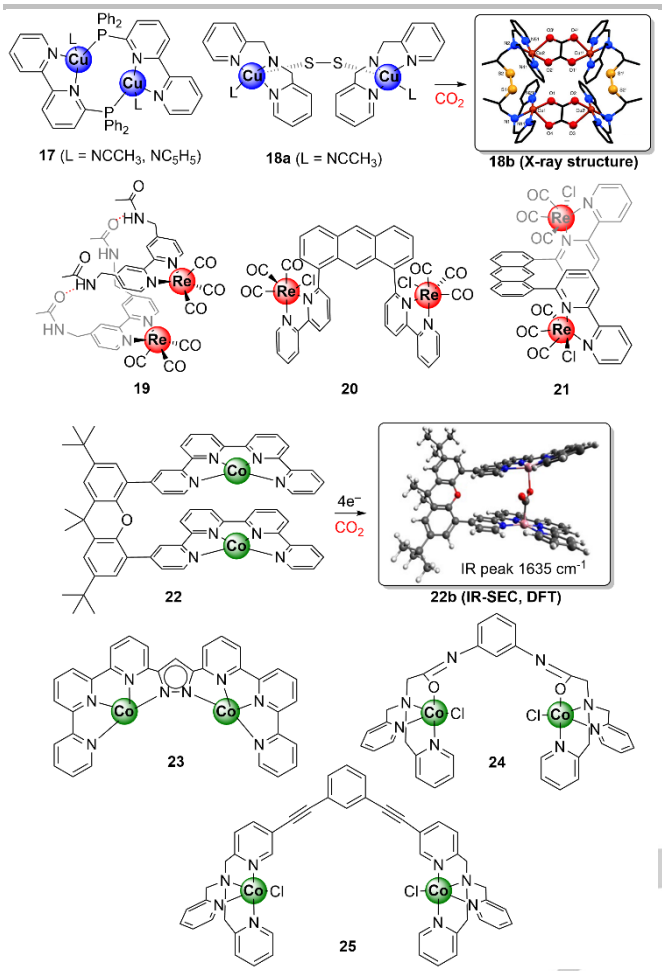

Figure 3. Polypyridyl ligand based homobimetallic catalysts. Structure 18B reproduced from Ref. 54, Copyright © 2010, The American Association for the Advancement of Science. Structure 22B reproduced from Ref. 61, Copyright © 2019, under exclusive license to Springer Nature Limited.

The advent of electrocatalytic performance of bipyridyl carbonyl based Re and Mn complexes for CO_2 reduction from the group of Lehn,[56] also made it possible to explore the bimetallic strategy. The group of Kubiak reported a hydrogen-bonded supramolecular Re dimer (catalyst **19**) formed *in situ* when mixing catalysts with acetoamidomethyl-modified bipyridyl ligands.[57] This dimer operated at 250 mV lower overpotential compared to the monomeric catalyst but still suffered from a low TOF and FE. Similar hydrogen-bonded Re dimer was reported when using amino acid residues (tyrosine or phenylalanine)[58] extending the flexible control of the metal center distance. A more rigid Re dimer was reported by the group of Jurss with anthracene as a bridge to maintain good distances between the metal centers (catalysts **20**-**21**).[59] Electrochemical studies show distinct mechanisms for two isolated isomers of the dimers: the *cis* conformer (catalyst **20**) works via a cooperative bimetallic CO_2 activation and conversion while the *trans* conformer (catalyst **21**) reduces CO_2 on a single-site, via a bimolecular pathway. DFT calculations show that the Re-Re distance in catalyst **20** is 3.4 Å, not too short to avoid formation of Re-Re bond but sufficient to activate a CO_2 molecule. Higher catalytic rates are observed for the *cis* conformer (TOF of 35 s^{-1}) relative to the *trans* conformer (TOF of 23 s^{-1}), outperforming the monomeric Re catalyst (TOF of 11 s^{-1}). Similar trends were observed when the catalysts were compared in photocatalytic regime using 1,3-dimethyl-2-phenylbenzimidazoline (BIH) as sacrificial electron donor.[60]

The group of Lau and Robert have reported a bimetallic cobalt quaterpyridine catalyst **22** linked by a xanthene bridge that shows photocatalytic reduction of CO_2 to either CO or formate depending on reaction conditions.[61] In an acetonitrile medium with Ru phenanthroline PS, selective production of formate (97%) with a TON of 386 was achieved when adding triethylamine (TEA) while CO was favored when phenol was added yielding 96% selectivity and TON of 829. The bimetallic cooperativity was supported by the much better activity compared to the monometallic analogue (TON_{HCOOH} of 96 under similar conditions). More importantly, infrared spectroelectrochemistry (IR-SEC) evidenced an absorption band at 1635 cm^{-1} corresponding to a stable adduct between CO_2 and the four-electron reduced catalyst (structure **22b**). Two electrons are located on one Co metal, which acts as nucleophile to bind the C atom of CO_2, one electron is on the second Co metal acting as an electrophile to stabilize one O atom of CO_2, and the fourth electron is delocalized over the ligand.

Recently, a dicobalt catalyst with terpyridine ligands linked by a pyrazole unit was reported by the same group (catalyst **23**).[62] The catalyst showed selective electrocatalytic reduction of CO_2 to CO in DMF with 1.5 M trifluoroethanol at −1.1 V *vs* NHE. However, it suffered from low FE of 39 %, deviating from the better performance of monometallic Co quaterpyridines, possibly indicating non-innocent role of the pyrazole linker. The distance between the two cobalt centers appears to play a crucial role in the intended cooperativity. No synergistic effects were observed for catalyst **24** with *meta* phenyl bridge resulting to a Co-Co distance of 5.8 Å (based on X-ray structure).[63] Though the catalyst showed a TON of 2600 and 97% CO selectivity with Ru phenanthroline PS and triethanolamine (TEOA) SED in CH_3CN with 11 M H_2O, it did not significantly differ from the monometallic analogue. A longer Co-Co distance of 14.8 Å (based on DFT) in catalyst **25** with rigid *meta* phenyl alkynyl bridge similarly showed no synergistic effect.[64] A TON of 360 and 92% CO selectivity was achieved using $Ir(ppy)_3$ PS and TEA SED in DMF, which is not significantly different from the monometallic analogue when normalized to the same metal concentration.

3.1.4. Porphyrin based catalysts

Even though the activity of metalloporphyrin catalysts towards electrochemical reduction of CO_2 was first reported in 1979 by the group of Toshima[65] and extensively optimized and mechanistically probed by the group of Savéant,[66,67] it was only in 2003 that the bimetallic activation using this ligand was reported by the group of Yamamoto.[68] A cofacial metalloporphyrin was self-assembled using electrostatic interactions between a cationic methylpyridylphenyl porphyrin and an anionic sulfonatophenyl porphyrin (catalyst **26**, Figure 4). Catalytic CO_2 reduction activity at −1.80 V *vs* Ag/Ag^+, forming CO and formaldehyde, with traces of H_2 (no quantification data available) was reported. The activity was attributed mostly to the Co cationic porphyrin unit while the anionic counterpart is assumed to act only as an electron mediator given its lack of activity under CO_2 in a control experiment.

More systematic studies were elegantly presented by the group of Naruta with cofacial iron porphyrins rigidly linked through different phenyl spacers (catalyst **27**).[69] Controlling the positioning of the porphyrin moieties in the phenyl linker (either in

the *ortho* or *meta* positions), made it possible to control the distance and the angle between the Fe porphyrins. An *ortho* configuration (**27a-*ortho***) expected to display a 3.2 – 4.0 Å Fe-Fe distance was suitable for activating the CO_2 substrate. This resulted in a higher catalytic activity (TOF of 2 × 10^4 s^{-1}, FE_{CO} of 95%, overpotential of 0.71 V) compared to the monomeric catalyst, thus showing a synergistic cooperativity between the two Fe metals.

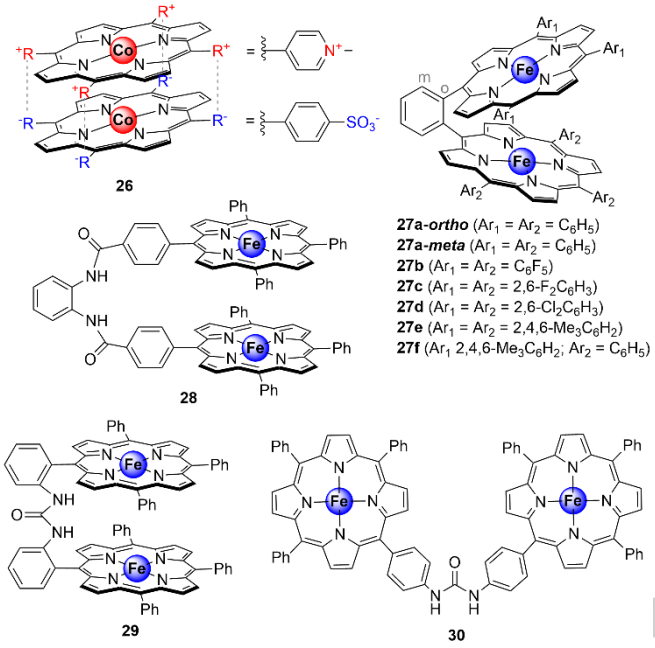

Figure 4. Porphyrin ligand based homobimetallic catalysts.

The performance of the catalyst was further optimized using through-structure electronic effects (catalysts **27b-f**).[70] Introducing electron-withdrawing substituents on the phenyl rings of the porphyrin (30 fluorine atoms in catalyst **27b**) lowers the catalytic overpotential to 0.56 V while maintaining a similar reaction rate constant. This breaks the electronic linear trend observed for monoporphyrin derivatives with substituted fluorophenyl groups (*i.e.,* decrease of rate constant when overpotential is lowered),[67] further demonstrating the synergistic effect of the two metals. Introducing electron donating groups (6 mesityl groups in catalyst **27e**), on the other hand, resulted in higher catalytic activity (TOF of 6 × 10^5 s^{-1}) at the cost of a higher overpotential (η = 0.91 V). Catalyst **27b** was even shown to keep its good CO selectivity in aqueous media when immobilized on SnO_2 or TiO_2 coated fluorine-doped tin oxide (FTO) cathodes.[71]

Cyclic voltammetry (CV) studies show overlapping stepwise reductions of the two iron porphyrin platforms, with the onset of the catalytic activity corresponding to the $Fe^{I/0}$ redox couple, indicating either the [$Fe^{I}Fe^{I}$] or [$Fe^{I}Fe^{0}$] to be the active species. For catalyst **27f** having different electronic environment around the Fe metals, a clear separation of the stepwise reductions was observed, and a strong catalytic current occurred at the onset potential of the [$Fe^{I}Fe^{0}$] species. This was assumed to indicate that probably Fe^{0} acts as a Lewis base and Fe^{I} acts as a Lewis acid in this bimetallic configuration. Given that the Lewis acid should maintain its Fe^{I} state during/after the catalytic cycle, it is difficult to distinguish the attributed Lewis acid role from this CV measurement alone.

Recently, the same group have reported a more flexible cofacial dimer with 1,2-phenylene amide bridge in catalyst **28**.[72] Compared to the overlapping redox couples of the rigid catalyst **27a**, this flexible catalyst resulted in a splitting into six redox waves, which the authors attributed to 'the long distance that electrons travel between the two Fe centers.' We believe that it is more plausible that the flexibility of the bridge assuming various orientations on the polarized electrode causes such an effect. The presence of the electron withdrawing amide functions substantially shifted the onset potential for CO_2 reduction to −0.9 V *vs* NHE, achieving a quite low overpotential of 0.15 V. Moreover, the catalytic activity (TOF of 2 × 10^7 s^{-1}) is substantially higher than the rigid catalyst **27a** (TOF of 6 × 10^2 s^{-1}) and monometallic analogue (TOF of 2 × 10^3 s^{-1}) under the same conditions, owing to the free movement of the porphyrin platforms to accommodate and convert the CO_2 substrate. Under heterogeneous conditions (adsorbed in Ketjen black carbon at glassy carbon, KBC@GC), catalyst **28** showed selective CO production in aqueous solution with current densities of 3.1 – 12.8 mA cm^{-2} at overpotentials of 0.26 – 0.46 V.

Inspired by the boosting effect of urea functions as multi-point hydrogen bond donors in iron porphyrins,[73,74] our group has synthesized an iron porphyrin dimer bridged by a urea group in one of the *ortho* phenyl positions (catalyst **29**)[75]. The crystal structure of the catalyst points to a good compromise between rigidity and flexibility as similarly assumed in catalyst **28**. Unlike catalyst **28**, catalyst **29** only showed three overlapping redox waves. Furthermore, CV of the homogeneous system points to no significant difference in the catalytic performances when compared to the monometallic analogue. The synergistic effect was only shown once the catalyst was adsorbed on multi-walled carbon nanotubes at carbon paper (MWCNT@CP) showing four times higher current density (while maintaining 89% FE_{CO}) than the monometallic iron porphyrin (with and without urea modification). The difference in the homogeneous performance in organic solvent and the heterogenized performance in aqueous solution relevantly points to differences in the rate-limiting step of the reaction mechanism. A similar iron porphyrin dimer but linked in the *para* position (catalyst **30**)[76] where the Fe centers are farther apart, showed only two times higher current density (with 89% FE_{CO}) than that of the monometallic iron porphyrin in heterogeneous conditions (MWCNT@GC). This highlights the importance of proper positioning of the two metal centers and the hydrogen bonding donor (urea group) within the catalytic pocket in a cofacial configuration (catalyst **29**).

3.1.5. Cryptate based catalysts

The concept and design of bimetallic cryptates (Figure 5) was initially reported by Lehn in 1980.[77] The group of Nelson showed that bimetallic octaazacryptates can incredibly fix atmospheric CO_2 as stable carbonates (catalyst **31**).[78] With systematic modifications of the spacer groups in Ni (II) cryptates (catalyst **32**), Apfel and colleagues even showed ability to fine tune CO_2 binding.[14,79]

It was only in 2017 that photocatalytic CO_2 reduction activity was reported by the group of Zhong and Lu for bimetallic Co cryptates (catalyst **33a**) together with Ru phenanthroline PS and triethanolamine (TEOA) SED in CH_3CN with 11 M H_2O.[80] A Co-Co distance of 5.8 Å was found to induce a synergistic effect of the two metals in displaying 98% CO selectivity and TOF of 0.47 s^{-1}, which is significantly higher than the monometallic analogue under the same conditions. The catalyst even maintained good

activity in dilute CO_2 conditions (10% in Ar) owing to its good CO_2 binding ability. The [$Co^{II}Co^{II}$] species captures the CO_2 substrate forming a carbonate cluster, but DFT suggests that the [$Co^{II}Co^{I}$] species reduces the substrate in a Lewis acid-base pair scheme.

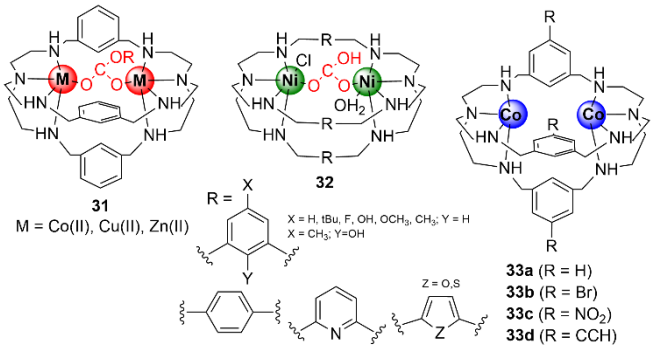

Figure 5. Cryptate ligand based homobimetallic catalysts.

The system was further optimized by the group of Martinho looking at the effects of substituents on the phenyl spacer (catalyst **33a-d**) on the photocatalytic activity.[81] Highest CO production rates of 1.32 s^{-1} with 95% selectivity were achieved with catalyst **33d** owing to the electron-donating nature of the ethyne substituents. Only when the specific Ru phenanthroline/TEOA combination was used as PS/SED couple the system was active. Interestingly, at longer irradiation times (30 h), CH_4 was produced with optimized activity in catalyst **33b** having 4% selectivity and TOF of 0.02 s^{-1}. [^{13}C]CH_4 was confirmed with [^{13}C]CO_2 catalysis experiments, however, it is concomitant with the deactivation of the catalysts at this long irradiation times.

3.1.6. Insights from homobimetallic design

The added value of the second metal in a homobimetallic design must be evaluated based on the synergistic effects (or lack of) and must be distinguished from the catalytic activity of the mononuclear unit acting independently. If looking only at the performance of parent monometallic catalyst, the comparison would be similar with those already reported in literature.[25,82–85] In this line, initial efforts on homobimetallic strategy have focused on developing dimers based on already established monometallic catalysts (*e.g.,* Ni cyclams, Fe porphyrins, Re bipyridyl triscarbonyl complexes, etc.). Thus, it seems that the critical factor controlling the cooperativity in these homobimetallic systems is the choice of the bridging linker. This choice affects (i) the distance between the two metal centers with the eventual accommodation of the CO_2 substrate, and (ii) the electronic communication between the two catalytic platforms that plays an additional role in the electron transfer process.

From the reports cited here, cooperative actions were observed for *ortho*-phenyl linkers in Ni cyclams and Fe porphyrins (catalysts **15a**, **27a**), rigid *cis*-configured anthracene bridge in Re bipyridyl catalysts (catalyst **20**), flexible cofacial dimer with 1,2-phenylene amide bridge (catalyst **28**), and the cryptate cages separated by *meta*-linked phenyl spacers (catalyst **33**). The compromise between rigidity and flexibility offered by these linkers must be systematically studied as synergistic effects might differ depending on how the catalytic platforms interact with each other. Importantly, the design of optimized bridging linkers may also include second coordination sphere effects such as hydrogen bond donors in catalyst **29** to further improve the catalytic performances, taking leverage of the growing efforts along this line.[24–27] Differing the roles of the two metal centers in this homobimetallic strategy has been systematically attempted by varying the electronic properties of each of the catalytic frameworks as shown by Naruta in catalyst **27**, but much more evident effects were observed employing different metal centers as will be discussed in the next chapter.

3.2. Heterobimetallic design

On the background of the different homobimetallic systems discussed, it is interesting to look at their heterobimetallic counterparts (Figure 6) especially since each of the metal centers is expected to play different roles in the activation and conversion of CO_2. Similar to the Ni-Fe metal centers in the CODH active site, one metal center is expected to act as the Lewis base pushing the electrons to the CO_2 substrate, while the other acts as Lewis acid to promote C-O bond cleavage. In this heterobimetallic case, there are even much fewer reports given the added synthetic complexity.

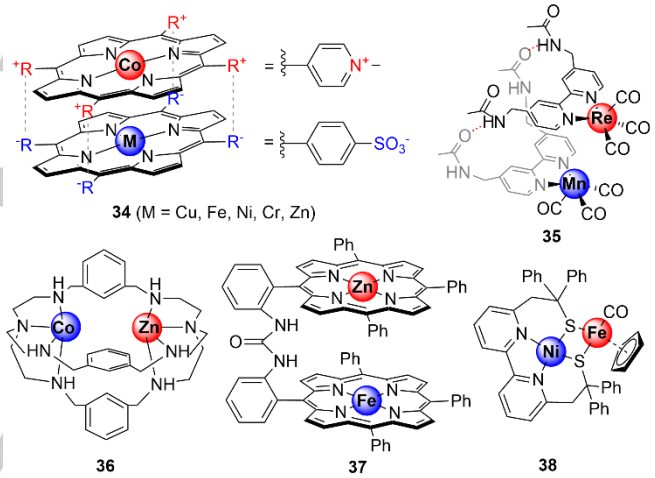

Figure 6. Heterobimetallic catalysts for CO_2 reduction.

The earliest report dated back to 2003 by the group of Yamamoto with cofacial Co-*M* (*M* = Cu, Fe, Ni, Cr, Zn) metalloporphyrins easily self-assembled through electrostatic interactions (catalyst **34**).[68] The Co-Cu dimer gave the highest limiting current in rotating disc voltammetry, which was much higher than that of the homobimetallic Co-Co catalyst **26**. Interestingly, switching to other metals (Fe, Ni, Cr, and Zn) in the anionic sulfonatophenyl porphyrin moiety resulted in a decrease of the limiting current. Unfortunately, no quantitative data (product amount, FE) was presented to solidify these claims and exert the heterobimetallic interactions toward CO_2.

The group of Kubiak utilized hydrogen-bonded supramolecular assembly to synthesize a heterobimetallic Re-Mn dimer (structure **35**) simply by mixing 1:1 equivalents of the Re- and Mn-centered acetoamidomethyl-modified ligands.[86] The mixture yielded a modest 10% current enhancement compared to homobimetallic Re-Re and Mn-Mn analogues, and bulk electrolysis experiments exhibited similar turnover numbers and a lower FE_{CO} of 86% (Mn-Mn at 100%). The heterobimetallic nature was probed with IR spectroelectrochemistry and it was proposed that the active species involves a doubly reduced Mn

metal that binds and activates the CO_2 substrate while the singly reduced Re metal transfers the electrons to the substrate.

With the cryptate ligand, the group of Zhong and Lu reported a heterometallic Co-Zn catalyst (Complex **36**) [87] which showed improved photocatalytic activity compared to its monometallic counterpart. This catalyst displayed a TOF of 1.8 s^{-1} and a 98% selectivity for CO when photosensitized by a Ru phenanthroline PS in the presence of TEOA. Control experiments with Co-Co and Zn-Zn dimers confirmed the synergistic effect of the non-identical metal centers. DFT calculations suggested that the Co (I) metal acts as the redox active site while the redox innocent Zn (II) metal, which has stronger affinity with OH^-, greatly promotes the C–OH cleavage in the O=C–OH intermediate.

Our group has also recently reported an Fe-Zn iron porphyrin dimer linked by a urea bridge (catalyst **37**).[75] Crystal structure of the catalyst evidenced a lateral shift of the cofacial porphyrin rings with an Fe-Zn distance of 6 Å. A water molecule is found bound to Zn, supporting the abovementioned affinity of Zn (II) metal towards OH^-. This heterobimetallic catalyst exhibited a similar catalytic activity in the heterogeneous state (MWCNT@CP) as the Fe-Fe homobimetallic analogue (catalyst **29**) even though the Zn porphyrin was shown to be catalytically incompetent. This brings clear support to the participation of both metal centers (Fe-Fe *vs* Fe-Zn) in the catalytic process but with differing modes of action. Though [Fe^0Fe^0] was deemed the active species based on CV, it seems that only one of the Fe metals is acting as Lewis base while the other acts as Lewis acid as similarly found for [Fe^0Zn^{II}]. The cooperativity may be favoring either the CO_2 binding or the C-O bond cleavage, identified as the possible rate determining step.

A closest functional mimic of the [NiFe] CODH was reported by the group of Artero, Dey, and Duboc with a heterobimetallic Ni-Fe catalyst **38** with bipyridyl-thiolate ligand.[88] The catalyst was initially reported as a bio-inspired model of the hydrogenase enzyme and was proven to be electrochemically active in H_2 production in acidic aqueous solutions.[89] The same catalyst was repurposed for CO_2 reduction. Once physisorbed on edge plane graphite electrode, electrolysis generated a mixture of H_2 (FE 66%) and CH_4 (FE 12%) as the products under optimal conditions (pH 4). The result is interesting with CH_4 being the sole C-containing product. [^{13}C]CO_2 experiments confirmed the origin of [^{13}C]CH_4 while electrolysis under CO atmosphere did not produce CH_4 indicating that CO is not an intermediate in the catalysis. Synergistic effect was evidenced by the lack of any CO_2 reduction activity from monometallic analogues (as well as from a closely resembling Ni-Fe bimetallic catalyst with Ni in S_4 environment compared to N_2S_2 in catalyst **38**). Even though no homogeneous electrocatalysis data has been shown, it was hypothesized from past reports that the Fe site is irreversibly poisoned by CO (inhibiting CO_2 reduction), but the Ni site actively transfers the needed hydride to CO until CH_4 is formed and released.

4. Summary and Outlook

In this review, we accounted for the bimetallic strategy of CO_2 activation in both enzymatic and artificial catalysts. Both share the molecular nature of the active site and provide a great avenue to understand the functioning of the natural catalysts and to implement the lessons learned in synthetic ones to control their performance. Knowledge of the catalytic mechanisms at work in a given system becomes rather crucial especially once these catalysts are heterogenized onto an electrode surface, where mechanistic studies are much more difficult. The variety of activity evaluations reported in electrocatalytic (homogeneous *vs* heterogenized) or photocatalytic regimes, and the unmatched trends and criteria in each regime make it difficult to present all comparisons in one single comprehensive plot. Nevertheless, one can make general observations, and from these, deduce some envisioned prospects.

(i) Bi(multi)metallic activation of small molecules (O_2, H_2O, CO_2, N_2, NO, *etc.*) in nature to manage multi electron and proton catalysis is a common feature together with the added importance of amino acid residues orchestrated in the proximity of the active sites that can provide both hydrogen bond donors and electrostatic activators. The exact roles of each of these features are yet to be firmly confirmed, but they provide a good basis to employ bio-inspired strategies in artificial systems.

(ii) The similarities in the structural features of CO dehydrogenases and enzymes that activate other small molecules (*e.g.,* hydrogenases for proton reduction), incorporating iron-sulfur clusters and typical metals such as Fe and Ni, may point to difficulties in distinguishing CO_2-activating processes from the competing proton reduction reaction within a strict biomimetic catalyst design. The fascinating chemistry of the biological reactions transforming CO_2 stems from the fact that the mechanisms of the enzyme-catalyzed reactions are clearly still different from the wide variety of synthetic bioinspired models. Indeed, once we have a better understanding of the biological reactions, chemists will be able to design synthetic catalysts that mimic the subtleties of biological catalysts.

(iii) There is a potential promise in bimetallic strategy for artificial catalyst design given that some reported systems here do not simply show additive properties of independent monometallic analogues. Careful design, however, is needed to control the topology between the metals and positioning them to establish proper activation and conversion of CO_2 possibly by finding the right compromise between ligand flexibility and rigidity. This has also been the core optimization strategy in supramolecular assemblies and porous cages to effect synergistic action on substrate capture, accumulation and activation within catalytic microenvironments.

(iv) Cofacial arrangements seem to generate synergistic improvement in these molecular bimetallic catalysts but are limited to a Lewis acid-base push-pull scenario, often giving a two-electron reduction product. To go towards further reduced products, bimetallic strategy must be reinvented, for example, having one metal as the active catalytic center for CO_2 and the other metal providing hydride in a tandem fashion. Similar to what is envisioned in heterogeneous catalysis, one metal can selectively reduce CO_2 to CO while the other metal selectively transforms CO further to a more reduced form. Along this line of thinking, the relevance of a cofacial arrangement must be re-evaluated for such tandem reactions.

(v) Though reports are rare, a heterobimetallic activation strategy seems to provide another level of control that homobimetallic catalysts lack. The limitations of synthetic complexity to achieve this can be resolved by efforts on isolating statistical combinations or by stepwise synthetic methodology, as has been presented in some reports here.

(vi) The advent and promise of rising trends in two-dimensional arrangement of catalysts in covalent organic

frameworks (COFs), polymeric chains, fused macrocycles, and three-dimensional arrangements in metal organic frameworks (MOFs) should be guided by similar learnings from bimetallic strategy to ensure that the repeating units are not just independently functioning in the system but synergistically working together. These frameworks often provide porosity for increased local substrate concentrations, but the catalytic units are often far apart, and leveraging close interactions between the two metal centers might provide opportunities for improved performance and/or offer alternate reaction pathways. This would especially be relevant to some of the bimetallic heterogeneous systems that have already been reported for various environmental applications (capture, sensing, purification, and conversion).

(vii) Systematic and control studies (*e.g.,* bimetallic *vs* monometallic, hetero- *vs* homo-bimetallic, new system *vs* state-of-the-art) are recommended to have accurate comparisons under the same experimental conditions. This makes it easier to establish structure-function relationships and performance trends. Further, this prevents and corrects any reproducibility issues from one report to another.

(viii) Though challenging, mechanistic insights through theoretical calculations and spectroscopy based (*ex situ, in situ, operando*) techniques are helpful to complement catalytic studies and re-evaluate design for further optimization. This is highly important to identify the actual active catalytic species generated from the initial pre-catalyst in a dynamic reaction microenvironment.

(ix) Combination of bimetallic strategy with second coordination effects (local proton sources, hydrogen bond donors, electrostatic activators) holds great promise as such combined effects are observed in natural systems (*e.g.,* NiFe-CODH). To determine whether or not the various combinations lead to synergistic effects will require careful studies as some combinations might have detrimental effects. Nevertheless, such studies will shed light on our understanding of the unmatched activities of enzymes and confirm whether we are overpraising or underestimating nature's tricks.

Acknowledgements

This work has been supported by the French National Research Agency (LOCO, grant N°: ANR-19-CE05-0020-02). We thank CNRS, CEA Saclay, ICMMO and University Paris-Saclay for the financial and research support. A. Aukauloo expresses gratitude to the Institut Universitaire de France for support.

Keywords: bimetallic complexes • bioinspired catalysis • carbon dioxide reduction • electrocatalysis • photocatalysis

[1] R. Kortlever, J. Shen, K. J. P. Schouten, F. Calle-Vallejo, M. T. M. Koper, *J. Phys. Chem. Lett.* **2015**, *6*, 4073–4082.

[2] M. Schreier, Y. Yoon, M. N. Jackson, Y. Surendranath, *Angew. Chem. Int. Ed.* **2018**, *57*, 10221–10225.

[3] M. K. Birhanu, M.-C. Tsai, A. W. Kahsay, C.-T. Chen, T. S. Zeleke, K. B. Ibrahim, C.-J. Huang, W.-N. Su, B.-J. Hwang, *Adv. Mater. Interfaces* **2018**, *5*, 1800919.

[4] S. Zhang, P. Kang, M. Bakir, A. M. Lapides, C. J. Dares, T. J. Meyer, *Proc. Natl. Acad. Sci. USA* **2015**, *112*, 15809–15814.

[5] C. Uyeda, J. C. Peters, *J. Am. Chem. Soc.* **2013**, *135*, 12023–12031.

[6] H. Cui, J. Wang, M. Hu, C. Ma, H. Wen, X. Song, C. Chen, *Dalton Trans.* **2013**, *42*, 8684–8691.

[7] D. Khusnutdinova, B. L. Wadsworth, M. Flores, A. M. Beiler, E. A. Reyes Cruz, Y. Zenkov, G. F. Moore, *ACS Catal.* **2018**, *8*, 9888–9898.

[8] W. Sinha, A. Mahammed, N. Fridman, Z. Gross, *ACS Catal.* **2020**, *10*, 3764–3772.

[9] Y. Feng, C. Wang, D. Bin, C. Zhai, F. Ren, P. Yang, Y. Du, *ChemPlusChem* **2016**, *81*, 93–99.

[10] L. Liu, A. Corma, *Chem. Rev.* **2023**, *123*, 4855–4933.

[11] C. Yang, Y. Men, Y. Xu, L. Liang, P. Cai, W. Luo, *ChemPlusChem* **2019**, *84*, 382–386.

[12] J. Zhao, J. Xu, J. Xu, J. Ni, T. Zhang, X. Xu, X. Li, *ChemPlusChem* **2015**, *80*, 196–201.

[13] K. E. Salnikova, Y. V. Larichev, E. M. Sulman, A. V. Bykov, A. I. Sidorov, G. N. Demidenko, M. G. Sulman, L. M. Bronstein, V. G. Matveeva, *ChemPlusChem* **2020**, *85*, 1697–1703.

[14] F. Möller, L. Castañeda-Losada, J. R. C. Junqueira, R. G. Miller, M. L. Reback, B. Mallick, M. van Gastel, U.-P. Apfel, *Dalton Trans.* **2017**, *46*, 5680–5688.

[15] R. Qiu, Z. Meng, S. Yin, X. Song, N. Tan, Y. Zhou, K. Yu, X. Xu, S. Luo, C.-T. Au, W.-Y. Wong, *ChemPlusChem* **2012**, *77*, 404–410.

[16] X. Xu, H. Lv, L. Sun, P. Song, B. Liu, X. Chen, *ChemPlusChem* **2020**, *85*, 970–976.

[17] L. Tang, G. Yu, X. Li, F. Chang, C.-J. Zhong, *ChemPlusChem* **2015**, *80*, 722–730.

[18] K. Sato, A. Ito, H. Tomonaga, H. Kanematsu, Y. Wada, H. Asakura, S. Hosokawa, T. Tanaka, T. Toriyama, T. Yamamoto, S. Matsumura, K. Nagaoka, *ChemPlusChem* **2019**, *84*, 447–456.

[19] K. R. Chithra, S. M. Rao, M. V. Varsha, G. Nageswaran, *ChemPlusChem* **2023**, *88*, e202200420.

[20] A. Tiwari, P. S. Sagara, V. Varma, J. K. Randhawa, *ChemPlusChem* **2019**, *84*, 136–141.

[21] Y. Zhou, B. Siang Yeo, *J. Mater. Chem. A* **2020**, *8*, 23162–23186.

[22] J. D. Goodpaster, A. T. Bell, M. Head-Gordon, *J. Phys. Chem. Lett.* **2016**, *7*, 1471–1477.

[23] E. Boutin, M. Robert, *Trends Chem.* **2021**, *3*, 359–372.

[24] P. Gotico, Z. Halime, A. Aukauloo, *Dalton Trans.* **2020**, *49*, 2381–2396.

[25] P. Gotico, W. Leibl, Z. Halime, A. Aukauloo, *ChemElectroChem* **2021**, *8*, 3472–3481.

[26] S. Amanullah, P. Saha, A. Nayek, M. E. Ahmed, A. Dey, *Chem. Soc. Rev.* **2021**, *50*, 3755–3823.

[27] J. N. H. Reek, B. de Bruin, S. Pullen, T. J. Mooibroek, A. M. Kluwer, X. Caumes, *Chem. Rev.* **2022**, *122*, 12308–12369.

[28] J.-W. Wang, D.-C. Zhong, T.-B. Lu, *Coord. Chem. Rev.* **2018**, *377*, 225–236.

[29] A. M. Appel, J. E. Bercaw, A. B. Bocarsly, H. Dobbek, D. L. DuBois, M. Dupuis, J. G. Ferry, E. Fujita, R. Hille, P. J. A. Kenis, C. A. Kerfeld, R. H. Morris, C. H. F. Peden, A. R. Portis, S. W. Ragsdale, T. B. Rauchfuss, J. N. H. Reek, L. C. Seefeldt, R. K. Thauer, G. L. Waldrop, *Chem. Rev.* **2013**, *113*, 6621–6658.

[30] V. Svetlitchnyi, C. Peschel, G. Acker, O. Meyer, *J. Bacteriol.* **2001**, *183*, 5134–5144.

[31] A. E. Boncella, E. T. Sabo, R. M. Santore, J. Carter, J. Whalen, J. D. Hudspeth, C. N. Morrison, *Coord. Chem. Rev.* **2022**, *453*, 214229.

[32] L. Grunwald, M. Clémancey, D. Klose, L. Dubois, S. Gambarelli, G. Jeschke, M. Wörle, G. Blondin, V. Mougel, *Proc. Natl. Acad. Sci. USA* **2022**, *119*, e2122677119.

[33] J.-H. Jeoung, H. Dobbek, *Science* **2007**, *318*, 1461.

[34] P. A. Lindahl, E. Münck, S. W. Ragsdale, *J. Biol. Chem.* **1990**, *265*, 3873–3879.

[35] H. Dobbek, L. Gremer, R. Kiefersauer, R. Huber, O. Meyer, *Proc. Natl. Acad. Sci. USA* **2002**, *99*, 15971–15976.

[36] B. Zhang, C. F. Hemann, R. Hille, *J. Biol. Chem.* **2010**, *285*, 12571–12578.

[37] M. Can, F. A. Armstrong, S. W. Ragsdale, *Chem. Rev.* **2014**, *114*, 4149–4174.

[38] S. Ciurli, P. K. Ross, M. J. Scott, S. B. Yu, R. H. Holm, *J. Am. Chem. Soc.* **1992**, *114*, 5415–5423.

[39] R. Panda, Y. Zhang, C. C. McLauchlan, P. Venkateswara Rao, F. A. Tiago de Oliveira, E. Münck, R. H. Holm, *J. Am. Chem. Soc.* **2004**, *126*, 6448–6459.
[40] D. Huang, R. H. Holm, *J. Am. Chem. Soc.* **2010**, *132*, 4693–4701.
[41] V. Artero, M. Fontecave, *Coord. Chem. Rev.* **2005**, *249*, 1518–1535.
[42] D. L. DeLaet, R. Del Rosario, P. E. Fanwick, C. P. Kubiak, *J. Am. Chem. Soc.* **1987**, *109*, 754–758.
[43] E. Simón-Manso, C. P. Kubiak, *Organometallics* **2005**, *24*, 96–102.
[44] D. L. DuBois, A. Miedaner, R. C. Haltiwanger, *J. Am. Chem. Soc.* **1991**, *113*, 8753–8764.
[45] B. D. Steffey, C. J. Curtis, D. L. DuBois, *Organometallics* **1995**, *14*, 4937–4943.
[46] J. W. Raebiger, J. W. Turner, B. C. Noll, C. J. Curtis, A. Miedaner, B. Cox, D. L. DuBois, *Organometallics* **2006**, *25*, 3345–3351.
[47] M. Beley, J.-P. Collin, R. Ruppert, J.-P. Sauvage, *J. Chem. Soc., Chem. Commun.* **1984**, *0*, 1315–1316.
[48] J. P. Collin, A. Jouaiti, J. P. Sauvage, *Inorg. Chem.* **1988**, *27*, 1986–1990.
[49] K. Mochizuki, S. Manaka, I. Takeda, T. Kondo, *Inorg. Chem.* **1996**, *35*, 5132–5136.
[50] C. de Alwis, J. A. Crayston, T. Cromie, T. Eisenblätter, R. W. Hay, Ya. D. Lampeka, L. V. Tsymbal, *Electrochim. Acta* **2000**, *45*, 2061–2074.
[51] L.-M. Cao, H.-H. Huang, J.-W. Wang, D.-C. Zhong, T.-B. Lu, *Green Chem.* **2018**, *20*, 798–803.
[52] S. Nitopi, E. Bertheussen, S. B. Scott, X. Liu, A. K. Engstfeld, S. Horch, B. Seger, I. E. L. Stephens, K. Chan, C. Hahn, J. K. Nørskov, T. F. Jaramillo, I. Chorkendorff, *Chem. Rev.* **2019**, *119*, 7610–7672.
[53] R. J. Haines, R. E. Wittrig, C. P. Kubiak, *Inorg. Chem.* **1994**, *33*, 4723–4728.
[54] R. Angamuthu, P. Byers, M. Lutz, A. L. Spek, E. Bouwman, *Science* **2010**, *327*, 313–315.
[55] F. Khamespanah, M. Marx, D. B. Crochet, U. R. Pokharel, F. R. Fronczek, A. W. Maverick, M. Beller, *Nat. Commun.* **2021**, *12*, 1997.
[56] J. Hawecker, J.-M. Lehn, R. Ziessel, *J. Chem. Soc., Chem. Commun.* **1984**, *0*, 328–330.
[57] C. W. Machan, S. A. Chabolla, J. Yin, M. K. Gilson, F. A. Tezcan, C. P. Kubiak, *J. Am. Chem. Soc.* **2014**, *136*, 14598–14607.
[58] C. W. Machan, J. Yin, S. A. Chabolla, M. K. Gilson, C. P. Kubiak, *J. Am. Chem. Soc.* **2016**, *138*, 8184–8193.
[59] W. Yang, S. Sinha Roy, W. C. Pitts, R. L. Nelson, F. R. Fronczek, J. W. Jurss, *Inorg. Chem.* **2018**, *57*, 9564–9575.
[60] N. P. Liyanage, W. Yang, S. Guertin, S. S. Roy, C. A. Carpenter, R. E. Adams, R. H. Schmehl, J. H. Delcamp, J. W. Jurss, *Chem. Commun.* **2019**, *55*, 993–996.
[61] Z. Guo, G. Chen, C. Cometto, B. Ma, H. Zhao, T. Groizard, L. Chen, H. Fan, W.-L. Man, S.-M. Yiu, K.-C. Lau, T.-C. Lau, M. Robert, *Nat. Catal.* **2019**, *2*, 801–808.
[62] A. Bohn, J. J. Moreno, P. Thuéry, M. Robert, O. Rivada-Wheelaghan, *Chem. Eur. J.* **2023**, *29*, e202202361.
[63] L. Zhang, S. Li, H. Liu, Y.-S. Cheng, X.-W. Wei, X. Chai, G. Yuan, *Inorg. Chem.* **2020**, *59*, 17464–17472.
[64] W. Xia, Y.-Y. Ren, J. Liu, B.-Y. Deng, F. Wang, *J. Photochem. Photobiol. A* **2022**, *426*, 113754.
[65] K. Takahashi, K. Hiratsuka, H. Sasaki, S. Toshima, *Chem. Lett.* **1979**, *8*, 305–308.
[66] M. Hammouche, D. Lexa, J. M. Savéant, M. Momenteau, *J. Electroanal. Chem. Interfacial Electrochem.* **1988**, *249*, 347–351.
[67] C. Costentin, J.-M. Savéant, *Nat. Rev. Chem.* **2017**, *1*, 0087.
[68] O. Enoki, T. Imaoka, K. Yamamoto, *Macromol. Symp.* **2003**, *204*, 151–158.
[69] E. A. Mohamed, Z. N. Zahran, Y. Naruta, *Chem. Commun.* **2015**, *51*, 16900–16903.
[70] Z. N. Zahran, E. A. Mohamed, Y. Naruta, *Sci. Rep.* **2016**, *6*, 24533.
[71] E. A. Mohamed, Z. N. Zahran, Y. Naruta, *Chem. Mater.* **2017**, *29*, 7140–7150.
[72] E. A. Mohamed, Z. N. Zahran, Y. Naruta, *J. Mater. Chem. A* **2021**, *9*, 18213–18221.
[73] P. Gotico, B. Boitrel, R. Guillot, M. Sircoglou, A. Quaranta, Z. Halime, W. Leibl, A. Aukauloo, *Angew. Chem. Int. Ed.* **2019**, *58*, 4504–4509.
[74] P. Gotico, L. Roupnel, R. Guillot, M. Sircoglou, W. Leibl, Z. Halime, A. Aukauloo, *Angew. Chem. Int. Ed.* **2020**, *59*, 22451–22455.
[75] C. Zhang, P. Gotico, R. Guillot, D. Dragoe, W. Leibl, Z. Halime, A. Aukauloo, *Angew. Chem. Int. Ed.* **2023**, *62*, e202214665.
[76] M. Abdinejad, C. Dao, B. Deng, M. E. Sweeney, F. Dielmann, X. Zhang, H. B. Kraatz, *ChemistrySelect* **2020**, *5*, 979–984.
[77] Lehn J.-M., *Pure Appl. Chem.* **1980**, *52*, 2441.
[78] Y. Dussart, C. Harding, P. Dalgaard, C. McKenzie, R. Kadirvelraj, V. McKee, J. Nelson, *J. Chem. Soc., Dalton Trans.* **2002**, *0*, 1704–1713.
[79] F. Möller, K. Merz, C. Herrmann, U.-P. Apfel, *Dalton Trans.* **2016**, *45*, 904–907.
[80] T. Ouyang, H.-H. Huang, J.-W. Wang, D.-C. Zhong, T.-B. Lu, *Angew. Chem. Int. Ed.* **2017**, *56*, 738–743.
[81] S. Realista, J. C. Almeida, S. A. Milheiro, N. A. G. Bandeira, L. G. Alves, F. Madeira, M. J. Calhorda, P. N. Martinho, *Chem. Eur. J.* **2019**, *25*, 11670–11679.
[82] K. E. Dalle, J. Warnan, J. J. Leung, B. Reuillard, I. S. Karmel, E. Reisner, *Chem. Rev.* **2019**, *119*, 2752–2875.
[83] C. Jiang, A. W. Nichols, C. W. Machan, *Dalton Trans.* **2019**, *48*, 9454–9468.
[84] R. Francke, B. Schille, M. Roemelt, *Chem. Rev.* **2018**, *118*, 4631–4701.
[85] H. Takeda, C. Cometto, O. Ishitani, M. Robert, *ACS Catal.* **2017**, *7*, 70–88.
[86] C. W. Machan, C. P. Kubiak, *Dalton Trans.* **2016**, *45*, 15942–15950.
[87] T. Ouyang, H.-J. Wang, H.-H. Huang, J.-W. Wang, S. Guo, W.-J. Liu, D.-C. Zhong, T.-B. Lu, *Angew. Chem. Int. Ed.* **2018**, *57*, 16480–16485.
[88] M. E. Ahmed, S. Adam, D. Saha, J. Fize, V. Artero, A. Dey, C. Duboc, *ACS Energy Lett.* **2020**, 3837–3842.
[89] M. E. Ahmed, S. Chattopadhyay, L. Wang, D. Brazzolotto, D. Pramanik, D. Aldakov, J. Fize, A. Morozan, M. Gennari, C. Duboc, A. Dey, V. Artero, *Angew. Chem. Int. Ed.* **2018**, *57*, 16001–16004.

Entry for the Table of Contents

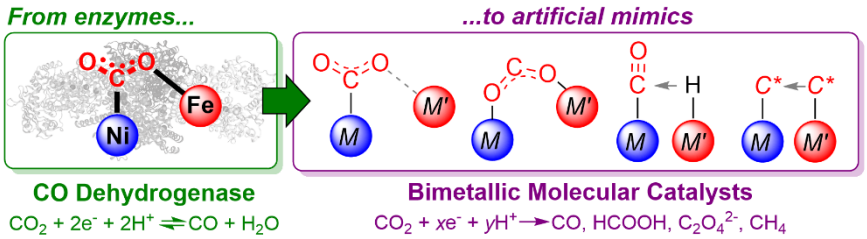

The challenge of developing catalysts for converting carbon dioxide CO_2 involves controlling its complex reaction pathways. Bimetallic cooperativity is a strategy that utilizes two metal centers to activate and convert CO_2. This review explores natural CO_2-activating enzymes and bio-inspired CO_2 reduction molecular catalysts that leverage such bimetallic strategy.

Institute and/or researcher Twitter usernames: @CEA_Joliot, @I2BCParisSaclay, @UnivParisSaclay